J Neurophysiol 92: 780–789, 2004;
10.1152/jn.01171.2003.

Precision of Spike Trains in Primate Retinal Ganglion Cells

V. J. Uzzell[1,2] and E. J. Chichilnisky[1,2]

[1]The Salk Institute, La Jolla 92037; and [2]University of California, San Diego, California 92037

Submitted 8 December 2003; accepted in final form 22 February 2004

Uzzell, V. J. and E. J. Chichilnisky. Precision of spike trains in primate retinal ganglion cells. *J Neurophysiol* 92: 780–789, 2004; 10.1152/jn.01171.2003. Recent studies have revealed striking precision in the spike trains of retinal ganglion cells in several species and suggested that this precision could be an important aspect of visual signaling. However, the precision of spike trains has not yet been described in primate retina. The spike time and count variability of parasol (magnocellular-projecting) retinal ganglion cells was examined in isolated macaque monkey retinas stimulated with repeated presentations of high contrast, spatially uniform intensity modulation. At the onset of clearly delineated periods of firing, retinal ganglion cells fired spikes time-locked to the stimulus with a variability across trials as low as 1 ms. Spike count variance across trials was much lower than the mean and sometimes approached the minimum variance possible with discrete counts, inconsistent with Poisson statistics expected from independently generated spikes. Spike time and count variability decreased systematically with stimulus strength. These findings were consistent with a model in which firing probability was determined by a stimulus-driven free firing rate modulated by a recovery function representing the action potential absolute and relative refractory period.

INTRODUCTION

Precise spike timing in the visual system may be important for representing time-varying stimuli, sensing motion, and other functions. Some stimuli have been shown to evoke spike time variability across trials as low as a few milliseconds in the retinas of salamander, rabbit, and cat (Berry and Meister 1998; Berry et al. 1997; Keat et al. 2001; Reich et al. 1997) and in the cat lateral geniculate nucleus (LGN) (Keat et al. 2001; Liu et al. 2001; Reich et al. 1997; Reinagel and Reid 2000, 2002). In addition, spike count variability in these species is considerably lower than expected from Poisson statistics (Berry and Meister 1998; Berry et al. 1997; Kara et al. 2000; Keat et al. 2001; Liu et al. 2001). These findings raise the possibility that visual information is transmitted to the brain in the precise times of individual action potentials rather than the firing rate averaged over tens or hundreds of milliseconds.

However, the relevance of these results for the primate visual system remains unclear because spike timing precision has not yet been examined in the primate retina or LGN (however, see Croner et al. 1993; Sun et al. 2004). Most studies of central visual system function are performed in primates because of close parallels with the human visual system. Thus determining the precision of the underlying retinal signals, which imposes a limit on the accuracy of visual performance, is fundamental. For example, spike time variability as low as 3 ms reported in extrastriate cortex (Bair and Koch 1996; Buracas et al. 1998) could reflect the precision of retinal spike trains or alternatively could require pooling of many less precise retinal inputs. Also, the high spike count variability observed in primate visual cortex (Bair and O'Keefe 1998; Barberini et al. 2000; Buracas et al. 1998; Gershon et al. 1998; McAdams and Maunsell 1999; Oram et al. 1999; Shadlen and Newsome 1998; Snowden et al. 1992; Softky and Koch 1993; Vogels et al. 1989) could be inherited from the retina or could reflect noise in downstream circuits. Precision in the retina may be a major constraint on central visual processing, such as the acute capacity of neurons in the cortex to sense visual motion based on the relative timing of spike trains in non-direction-selective inputs. The much higher maintained firing rate of primate retinal ganglion cells compared with those of some nonprimate species raises the possibility that spike train precision is also different, which could have significant consequences for central visual function.

In this paper we examine spike time and count variability of primate parasol, or magnocellular-projecting, retinal ganglion cells (RGCs) elicited by time-varying spatially uniform stimuli. At the onset of clearly delineated periods of firing, spike time variability as low as 1 ms was observed, similar to findings in the retina and LGN of other species and in primate visual cortex. The variance of spike counts across trials was significantly lower than expected from Poisson statistics, was lower than values reported in primate visual cortex, and was similar to values reported in the retinas of other species. Spike time and count variability decreased with stimulus strength, and were somewhat lower in ON cells than OFF cells. The observed spike time and count variability could be explained by a model in which firing is controlled by a stimulus-dependent free firing rate modulated by action potential refractoriness. These data provide a summary of spiking statistics in primate retina and a benchmark for understanding how these statistics may contribute to central visual function.

METHODS

Preparation

Eyes were obtained from terminally anesthetized macaque monkeys (*Macaca fascicularis, M. mulatta, M. radiata*) used by other experimenters in accordance with institutional guidelines for the care and use of animals. Immediately after enucleation, the anterior portion of the eye and vitreous were removed in room light, and the eye cup was placed in bicarbonate-buffered Ames' solution (Sigma, St. Louis, MO) and stored in darkness for ≥20 min before dissection. Under infrared illumination, pieces of retina 2–4 mm in diameter were cut from regions 6–11 mm from the fovea (temporal equivalent eccentricity, Chichilnisky and Kalmar 2002); in one experiment, the eccentricity was unknown. The retina was placed flat against a planar array

Address for reprint requests and other correspondence: E. J. Chichilnisky, Systems Neurobiology, The Salk Institute, 10010 North Torrey Pines Rd., La Jolla, CA 92037 (E-mail: ej@salk.edu).

The costs of publication of this article were defrayed in part by the payment of page charges. The article must therefore be hereby marked "*advertisement*" in accordance with 18 U.S.C. Section 1734 solely to indicate this fact.

of 61 extracellular microelectrodes that were used to record action potentials from retinal ganglion cells (Chichilnisky and Baylor 1999; Meister et al. 1994). The retina was superfused with Ames' solution bubbled with 95% O_2–5% CO_2 and maintained at 32–36° C (pH 7.4). In all experiments, the retinal pigment epithelium was left attached to the retina during recording.

Recordings

Spike times, peaks, and widths were digitized at 20 kHz (Litke 1999; Meister et al. 1994) and stored for off-line analysis. Spikes from 10 to 50 cells were segregated by manually selecting distinct clusters in scatter plots of spike height and width recorded on each electrode and verifying the presence of a refractory period in the spike trains from each cluster. Only well-isolated clusters with low contamination were chosen for further analysis. For each cell, contamination was defined as the average spike rate in the period 0.5–1.0 ms following recorded spikes divided by the average overall spike rate. Most cells analyzed (80%) exhibited contamination <1%, and all exhibited contamination <7%. Spikes recorded on multiple electrodes were identified by temporal coincidence; only spikes from the electrode with the most clearly defined cluster were retained. Cells or segments of experiments that exhibited obvious instability in firing rate were excluded from analysis. The plots in Figs. 1, 2, 4, 7, and 8 were obtained from cells selected for contamination lower than 0.25% and for firing rates in the middle of the range observed in ON or OFF cells in the same retina.

Stimuli

The retina was stimulated with the optically reduced (1.0–1.3 mm diam) image of a cathode ray tube computer display refreshing every 8.33 ms (4 experiments) or 15 ms (1 experiment), focused on the photoreceptor layer by a microscope objective, and centered on the 480-μm-diam electrode array. The stimulus was delivered from the retinal ganglion cell side through the mostly transparent electrode array. The shadows cast by the platinized (opaque) electrode tips, 5 μm in diameter and spaced 60 μm apart, had a minimal influence on the intensity and spatial pattern of the stimulus, because they occupied ~1% of the total area of the array and were optically diffused by virtue of lying in a different focal plane than the photoreceptors. Most cells showed no time-locking to the monitor refresh: for only 2 of 41 cells was periodicity at the monitor refresh rate observed in the autocorrelation function.

The stimulus was a spatially uniform display that assumed one of two intensity values, randomly selected on every frame. The temporal contrast of the stimulus (96% in 3 experiments, 80% in 1 experiment, and 48% in 1 experiment) was defined as the SD of the intensity divided by the mean. A single random stimulus sequence 8–30 s long was presented repeatedly (19–176 times in different experiments). The mean photon absorption rate caused by the stimulus in the long-, middle-, and short-wavelength-sensitive cones was approximately equal to the absorption that would have been caused by spatially uniform monochromatic lights of wavelength 564, 534, and 432 nm and intensities of 3,850–15,030, 3,770–14,740, and 2,020–7,900 photons–μm^{-2}–s^{-1}, respectively (values indicate range across experiments).

Cell types

Analysis was restricted to two physiologically defined classes of cells that very likely correspond to ON and OFF parasol cells (Polyak 1941) based on several lines of evidence (Chichilnisky and Kalmar 2002). First, in each retina, the collection of ON and OFF cells each appeared to comprise a single cell type based on their receptive field diameters and tiling and response rasters. Receptive field diameters were computed from the spike triggered average stimulus obtained with spatio-temporal white noise (Chichilnisky 2001; Chichilnisky and Kalmar 2002). Second, the receptive field diameters of all cells were consistent with the predicted receptive field diameters of parasol cells at the same eccentricity. In some data sets, a second group of cells was identified with receptive field diameters consistent with those of midget cells at the same eccentricity. These cells were excluded from analysis because their spikes were usually not well isolated.

Analysis of spike time variability

Spike time variability was measured at points in the spike train that followed clearly defined periods of inactivity, determined as follows. The cross-correlation function between the spike train in the first trial and spike trains in all subsequent trials was computed over the range ±50 ms. The least-squares fit of a Gaussian function, $f(x) = k + a \cdot \exp(-x^2/2\sigma^2)$, to the cross-correlation function was obtained, and the correlation time was defined as $2\sigma\sqrt{2}$. This indicates the average time scale of reproducibility of the light response. Periods of firing following inactivity longer than a correlation time were identified as candidates for timing variability analysis.

A simple measure of spike time variability at such points in the spike train would be the SD of the time to the first spike. However, this measure is confounded by unreliability, an example of which occurs following the end of a period of inactivity at 0.88 s in Fig. 1*C* (left). In a small number of trials, the cell did not fire a spike within the time period defined by the roughly 10 ms wide vertical band of firing in the raster; instead, the next spike occurred much later (0.95–0.96 ms). Such outlying spikes probably represent the response to a different portion of the stimulus sequence and thus would distort estimates of variability of the earlier response. For this reason, previous studies have attempted to measure spike time variability in a way that accounted for unreliability (Berry et al. 1997; Keat et al. 2001; Liu et al. 2001; Reinagel and Reid 2000). In this study, this was accomplished as follows.

First, to eliminate cases in which a substantial fraction of spikes was obviously elicited by a different segment of the stimulus, spike time variability was not computed if >10% of trials contained no spikes within two correlation times following the period of inactivity. Second, to reduce the effects of remaining outliers, spike time variability was computed using a robust estimate of the SD. Let $\{t_i\}$ represent the set of first spike times across all trials and let med$\{t_i\}$ denote the median of this distribution. A robust estimate of the SD is $\sigma_r = \text{med}|t_i - \text{med}\{t_i\}|/0.674$ (Huber 1981). This was compared with the standard estimate, $\sigma_s = [\Sigma(t_i - \text{mean}\{t_i\})^2/(N-1)]^{1/2}$, as follows. Accuracy was tested on random samples from a Gaussian distribution with unit SD. Across 1,000 simulations with $n = 50$ samples each (typical number of trials), σ_s was in the range 0.99 ± 0.10 (SD), and σ_r was in the range 1.01 ± 0.17. Thus σ_r was reasonably accurate in the Gaussian case. Robustness was tested by replacing 10% of the N samples in each simulation with values drawn from a distribution with SD of 10. In this case, σ_s was in the range 3.2 ± 0.93, whereas σ_r was in the range 1.13 ± 0.19. Thus σ_r was much less sensitive to outliers.

To verify that use of the robust measure did not alter the main conclusions about the limits of spike time variability, variability was also computed using the standard measure σ_s. About 80% of cells recorded exhibited minimum spike time variability <2 ms, and ~10% exhibited minimum spike time variability <1 ms, qualitatively consistent with the findings reported in RESULTS using the measure σ_r.

Simulations

The statistics of recorded spike trains were compared with those of two models described below. In each case, the number of simulation trials was equal to the number of data trials. Simulated and real spike trains were discretized in 0.1-ms time bins. The time-varying firing rate $r(t)$ for each cell was estimated by computing the proportion of trials in which the cell fired a spike in each time bin.

In Poisson simulations, the time-varying rate $\lambda(t)$ of an inhomogeneous Poisson process was set to $r(t)$. For this Poisson process, the probability $P_t(k)$ of k spikes occurring in a bin at time t is

$$P_t(k) = \lambda(t)^k \exp[-\lambda(t)]/k!$$

However, for values of $\lambda(t) \ll 1$ obtained with small time bins, the probability that $k > 1$ is negligible, so a sample from a Poisson distribution can be approximated by a binary random draw, with $P_t(1) = \lambda(t)$ and $P_t(0) = 1 - P_t(1)$. Simulated spike trains were generated by setting the spike count in each time bin to the result of this random draw.

In refractory simulations, given that the previous spike occurred at time t_{last}, the spike rate $\lambda(t,t_{last})$ in each time bin was assumed to be the product of a free firing rate $q(t)$ and a recovery function $w(t - t_{last})$ (Berry and Meister 1998)

$$\lambda(t,t_{last}) = q(t)w(t - t_{last})$$

Here, the first term is the stimulus-dependent part of the response, and the second term captures the effects of refractoriness, which reduces the probability of firing for a brief period after a spike. To estimate the free firing rate $q(t)$, the probability that the cell was available for free firing $W(t)$ was calculated as follows. For the ith trial, the effect of refractoriness at time t is $W_i(t) = w(t - t_{last})$, where t_{last} represents the time of the last spike prior to t, and $W_i(t) = 1$ prior to the first spike. Then the expected effect of refractoriness across trials is given by

$$W(t) = \sum_{i=1}^{N} W_i(t)/N$$

where N is the number of trials. Given $W(t)$, the estimated free firing rate was $q(t) = r(t)/W(t)$. Simulated spike trains were generated by setting the spike count value in each time bin according to a binary random draw with $P_t(1) = \lambda(t,t_{last})$.

The recovery function $w(t)$ for each cell was given by

$$w(t) = \frac{\lfloor t - t_{abs} \rfloor^p}{(\lfloor t - t_{abs} \rfloor^p + t_{rel}{}^p)}$$

where $\lfloor \cdot \rfloor$ represents clipping negative numbers to zero, t_{abs} is the absolute refractory period estimated from the spike train auto-correlation, t_{rel} is the half-saturating point selected to minimize the squared difference between the Fano factor (see RESULTS) computed from the data and the simulation, and p is a constant fixed at 4. Examples of recovery functions for two cells are shown in Figs. 7*B* and 8*B* (*bottom, inset*). The recovery function was estimated this way because the parameter-free method described previously (Berry and Meister 1998) assumed approximately binary firing rates.

RESULTS

Figure 1 shows spike rasters and time-varying firing rates obtained from a representative sample of eight parasol (magnocellular-projecting) RGCs, one ON cell and one OFF cell from each of four retinas, in response to repeated presentations of a spatially uniform randomly flickering stimulus. Under these conditions, RGCs were frequently driven to fire at rates in excess of 100 Hz, and responses were highly reproducible across trials. These stimulus conditions and responses resemble those used recently to explore spiking precision in salamander and rabbit RGCs (Berry et al. 1997) and cat LGN neurons (Keat et al. 2001; Reinagel and Reid 2000). To quantify the precision of primate RGC responses in these conditions, simple measures of spike time and count variability were employed.

Spike time variability

Spike timing precision was probed by examining the variability in the time of the first spike following a clearly delineated period of inactivity, as follows. Periods of inactivity (no spikes fired on any trial) longer than the correlation time of the light response were identified. The correlation time was defined as twice the width of a Gaussian function fitted to the cross-correlation between the spikes recorded in one trial and all others (see METHODS). This reflects the average timescale of evoked firing rate modulations. Across 41 cells in five retinas, the correlation time was 20 ± 7 ms (SD), comparable to the integration time of primate cones (Schnapf et al. 1990). In Fig. 1, the ends of several such periods of inactivity are marked with a dot on the time axis of the raster.

Spike time variability was examined by accumulating the time of the first spike following the period of inactivity across all trials and computing an estimate of the SD of these spike times. To suppress the upward bias on spike time variability caused by unreliable spiking, cases in which <90% of trials contained a spike within two correlation times following the end of the period of inactivity were excluded from analysis, and an estimate of the SD was used that suppressed the effects of outliers (see METHODS). This procedure provided a simple measure of spike time variability at points in the spike train where the onset of firing was easily identified and firing was reliable. At these time points, this measure resembles measures used in recent studies in other species (see DISCUSSION).

Figure 2 shows histograms of spike time variability for the same eight cells as Fig. 1. Timing variability was usually lower than 5 ms and sometimes as low as 1 ms. Figure 3, *A* and *B*, shows pooled data for all ON and OFF cells examined. While spike time variability varied considerably across stimuli and cells, values approaching 1 ms were observed often. Similar results were obtained using a definition of correlation time one-half and twice as large as the original definition.

ON cells exhibited somewhat lower spike time variability than OFF cells. This can be seen in Fig. 3*C*, which shows the histograms of Fig. 3, *A* and *B*, normalized to unit area and overlaid. The mean spike time variability for ON cells was 2.77 ms and for OFF cells was 3.68 ms ($P < 0.0001$, Wilcoxon rank-sum test; Rosner 1995). A similar asymmetry was observed by examining the median spike time variability for each cell separately: the mean of this value across ON cells was 2.42 and across OFF cells was 3.56 ($P = 0.016$, Wilcoxon rank-sum test).

Spike count variability

Spike count variability was examined by comparing the variance of spike counts across trials to the mean. Figure 4 shows the relationship between spike count variance and mean for the same eight cells as Fig. 1, in time bins of 10 ms. The diagonal line in each plot represents equality of variance and mean that would be expected from Poisson spike generation, in which the probability of a spike at any point in time depends only on the instantaneous firing rate and not on the times of previous spikes. Spike count variance was much lower than expected from Poisson statistics and often approached the minimum variance possible with discrete counts, shown by the scalloped line.

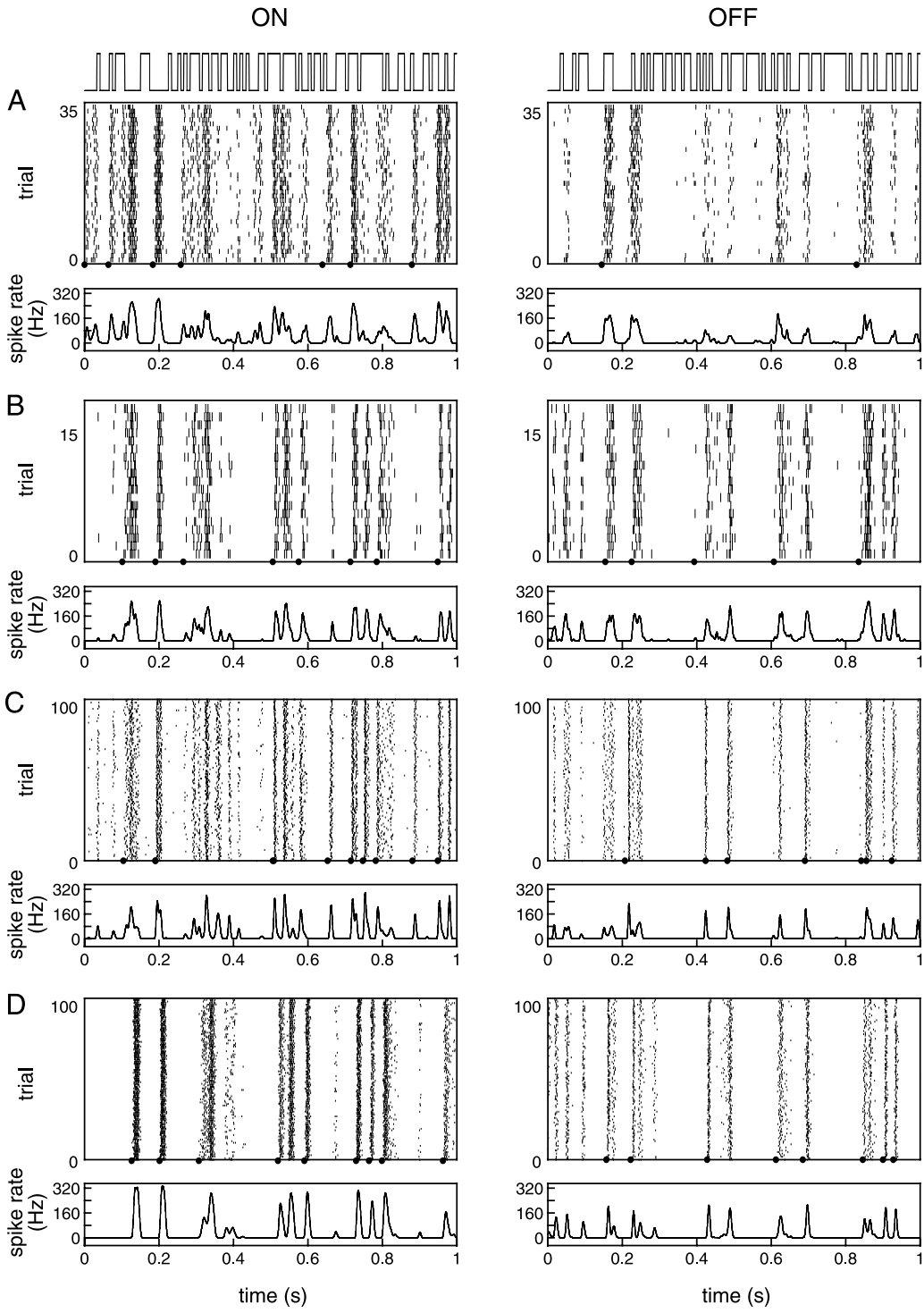

FIG. 1. Primate retinal ganglion cell firing patterns. Rasters and firing rates over time are shown for representative ON and OFF parasol cells from each of 4 retinas (*A*, *B*, *C*, and *D*, respectively). The stimulus was spatially uniform binary noise with time course shown above the rasters in *A*. The root mean square (RMS) stimulus contrast was 96, 80, 96, and 96%, respectively. The stimulus refresh interval was 8.33 ms. The dots on the time axis represent identified times of firing onset; periods with unreliable firing were excluded (see RESULTS). Beneath each raster, the time-varying firing rate is shown, calculated in 0.1-ms bins and smoothed by a Gaussian filter with a SD of 2 ms.

Figure 5, *A* and *B*, shows the dependence of spike count variability on mean pooled across all ON and OFF cells in five retinas. To quantify the deviations of the data from the Poisson prediction, the Fano factor (ratio of variance to mean) was estimated by linear regression of the variance against the mean for the pooled data. The Fano factor was 0.277 ± 0.002 (SE) for ON cells and 0.369 ± 0.003 for OFF cells. This difference could reflect higher firing rates in ON cells combined with the fact that the mean-variance relation is not linear or could reflect a difference in the mean-variance relation. This was examined by computing

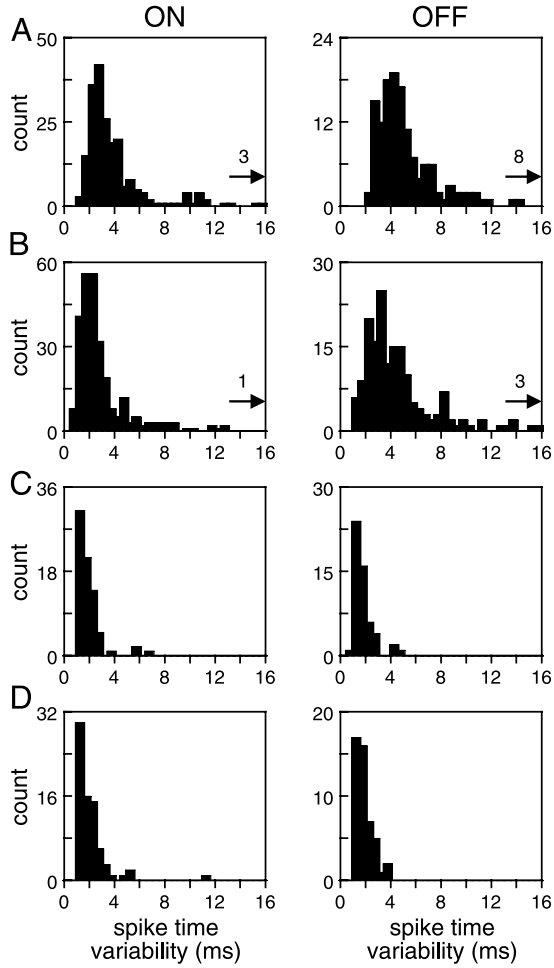

FIG. 2. Spike time variability. Each panel shows a histogram of spike time variability accumulated from various time points in the light response for the same cells and stimuli as Fig. 1. The value of the abscissa indicates the estimated SD across trials of the time to the 1st spike after a period of inactivity exceeding 1 correlation time, in 1-ms bins. Cases in which <90% of trials contained a spike within 2 correlation times of the end of inactivity were excluded, and a robust estimate of SD was used (see METHODS). *Inset:* number of values higher than the histogram abscissa range. Correlation times for ON and OFF cells—*A*: 23, 32 ms; *B*: 17, 28 ms; *C*: 12, 10 ms; *D*: 17, 8 ms. Stimulus duration—*A*: 30 s; *B*: 30 s; *C*: 8 s; *D*: 8 s. Number of trials—*A*: 37; *B*: 19; *C*: 176; *D*: 167.

spike count variance and mean averaged within each of 10 spike count mean bins, for ON and OFF cells separately; results are shown in Fig. 5*C*. OFF cells exhibited slightly higher spike count variance than ON cells ($P = 0.03$, Wilcoxon signed-rank test; Rosner 1995), particularly for large spike counts.

Dependence on stimulus strength

Spike time variability decreased systematically with the strength of the stimulus. This was determined by examining spike time variability and stimulus strength at different time points in the response. Stimulus strength was assessed by assuming that RGC firing at each point in time was determined by a weighted sum of recent contrast values. The weights for each cell were estimated by computing the spike-triggered average (STA) stimulus from a long white noise sequence. The effective contrast for each stimulus frame during the repeated stimulus sequence was then defined as the sum of recent contrast values multiplied by these weights. Effective contrast was interpolated between stimulus frames using a cubic spline. Effective contrast indicates the strength of the excitatory or inhibitory drive elicited by the stimulus (see Chichilnisky 2001). Spike time variability was examined as a function of the effective contrast occurring at the time of the median first spike following each identified period of inactivity. The relationship between spike time variability and effective contrast is shown in Fig. 6*A*, using pooled data from five ON cells and four OFF cells in one preparation. Higher effective contrast yielded progressively lower spike time variability.

Spike count variability also decreased with stimulus strength. This can be seen in the dependence of the Fano factor on effective contrast, shown in Fig. 6*B* for pooled data from the same cells. This dependence is expected due to the increased firing rate at higher contrast and the nonlinear form of the mean-variance relationship.

Refractory model of light response statistics

A model that incorporated the effects of action potential refractoriness approximately reproduced the spike time and count variability of RGC spike trains. Figure 7*A* shows rasters

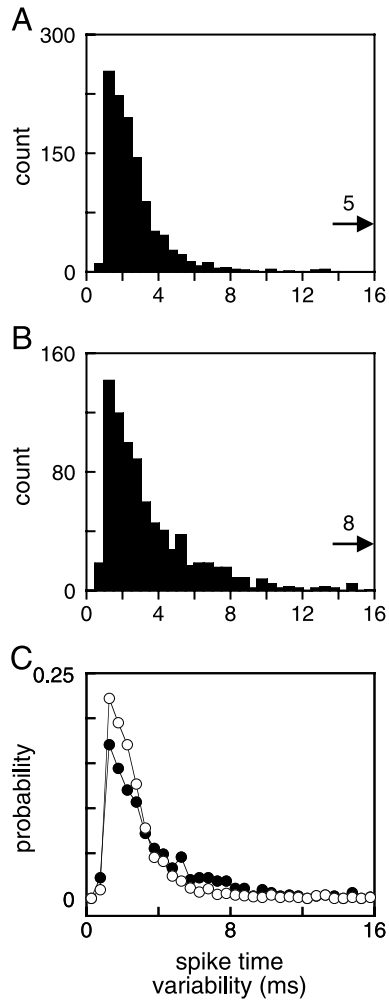

FIG. 3. Spike time variability summary. Histograms show the pooled distribution of spike time variability values accumulated across all 19 ON-parasol cells (*A*) and 22 OFF-parasol cells (*B*) recorded in 5 retinas, in 0.5-ms bins. Data were accumulated across 8 s of response for each cell; number of trials same as Fig. 2. *Inset*: number of values higher than the histogram abscissa range. In *C*, histograms from *A* and *B* normalized to unit area are overlaid for comparison. Open symbols represent ON cells; filled symbols represent OFF cells.

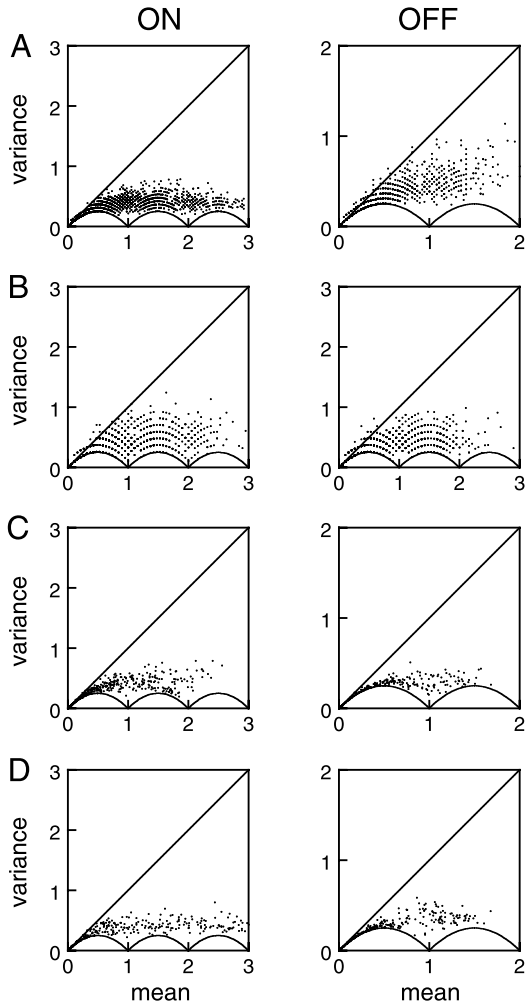

FIG. 4. Spike count variability. Each panel shows the relation between spike count variance and mean for a single cell. The location of each point indicates the variance and mean observed in 1 time bin of size 10 ms. The diagonal line represents equality of variance and mean expected from Poisson statistics. The scalloped line represents the minimum variance possible with discrete counts for a given mean. Minimum variance is given by $p(1 - p)$, where $p = m - n$, m is the mean count, and n is the largest integer such that $n < m$. Cells, stimulus duration, and number of trials same as Fig. 2.

of responses to repeated stimulation for an ON cell, a Poisson model with the same time-varying firing rate, and a refractory simulation in which the probability of firing was controlled by an underlying free firing rate multiplied by a recovery function which depended only on the time since the last spike (Berry and Meister 1998). The Poisson simulation produced a more variable pattern of firing from trial to trial than the data, while the refractory simulation produced a pattern of firing which resembled the data.

Figure 7*B* shows histograms of spike time variability computed from the data and the two simulations. The Poisson simulation exhibited spike time variability higher than that of real spike trains, whereas the refractory simulation exhibited variability comparable to the data. This may reflect the fact that in the presence of refractoriness, strong stimulus-driven inputs can essentially guarantee a spike on every trial within a short period while remaining consistent with the observed firing rate, but the inherently more stochastic Poisson process with the observed firing rate cannot. In addition, the Poisson simulation yielded a smaller number of cases in which the response was reliable enough to meet the criteria of the analysis, hence a smaller total count in the histograms.

Figure 7*C* shows spike count variability as a function of spike count mean for the data and the two simulations. The Poisson simulation exhibited spike count variance approximately equal to the mean, as expected. The spike count variability for the data was much lower, near the minimum variance curve. The refractory simulation produced a spike count variance to mean relationship similar to the data. This reflects the fact that refractoriness regularizes the number of spikes per unit time by making high spike counts less likely.

The refractory model provided a reasonably accurate description of the firing statistics of all RGCs recorded. Results similar to those of Fig. 7 are shown for a sample OFF cell in Fig. 8. Across 41 cells in five retinas, the linear regression coefficient relating the median spike time variability of each cell to

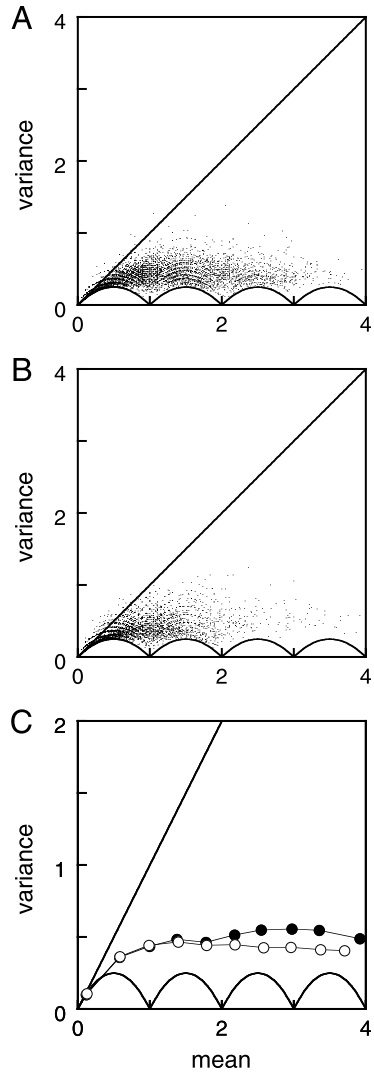

FIG. 5. Spike count variability summary. Spike count variance and mean were accumulated across all 10-ms time bins for 19 ON-parasol cells (*A*) and 22 OFF-parasol cells (*B*) recorded in 5 retinas. In *C*, the spike count variance and mean for ON cells (open symbols) and OFF cells (filled symbols) are overlaid for comparison. Each point in *C* was obtained by binning the spike count means in equal intervals and computing the average spike count variance and average spike count mean within each bin. Cells, stimulus duration, and number of trials same as Fig. 3.

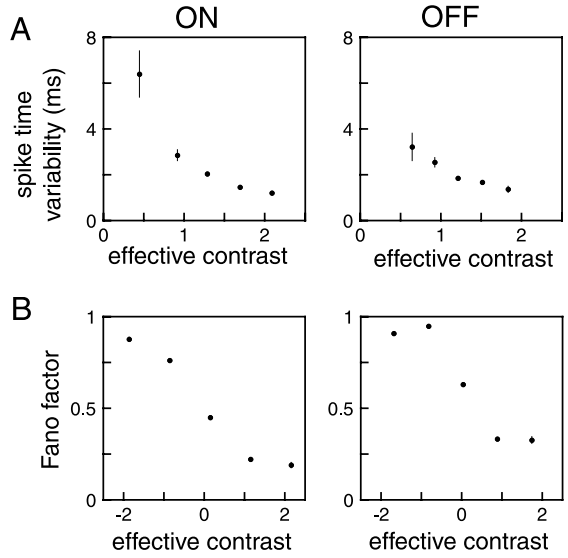

FIG. 6. Dependence of spike time and count variability on stimulus strength. (*A*) Spike time variability is shown as a function of effective contrast, pooled across 5 ON cells (left) and 4 OFF cells (right) from 1 retina. Effective contrast for each cell was defined as the correlation of the stimulus with the spike-triggered average (STA) computed over 167 ms (20 frames) preceding a spike (see RESULTS). Effective contrast was binned in equal intervals, and spike time variability for each bin was the mean across all time points for which effective contrast fell within the bin. Error bar represents SE. (*B*) Estimated Fano factor is shown as a function of effective contrast, pooled across the same cells as in *A*. Effective contrast was binned in equal intervals, and mean and variance of spike counts across all time points for which effective contrast fell within the bin were accumulated; the Fano factor was estimated using the regression of mean against variance. Error bars represent the SE of the regression coefficient. Spike counts were computed in time bins of size 8.33 ms (1 stimulus frame).

that of the simulation was 0.979; the correlation coefficient was 0.980. The corresponding regression and correlation coefficients relating the Fano factor of the simulation to the data were 1.00 and 0.998 (note: the Fano factor error was minimized in the selection of model parameters; see METHODS). For comparison, the regression coefficient relating the timing variability of the Poisson simulation to that of data was 1.35.

The refractory model also reproduced the asymmetry in ON and OFF cell spike time and count variability. The average across simulated ON cells of the median spike time variability for each cell was 2.33 ms; across simulated OFF cells this average was 3.44 ms ($P = 0.04$, Wilcoxon rank-sum test). The mean Fano factor for simulated ON cells was 0.296 and for simulated OFF cells was 0.423 ($P < 0.001$, Wilcoxon rank-sum test). Simulated OFF cells also showed greater spike count variability at a given firing rate than simulated ON cells, specifically at higher firing rates (data not shown).

DISCUSSION

Spike time variability in primate RGCs

Strong spatially uniform stimuli evoked precisely timed spikes in primate RGCs, with variability in the onset of firing often on the order of 1 ms. This value is as low as has been observed in any visual system neuron in any species, including salamander and rabbit RGCs, cat RGCs and LGN neurons, and primate visual cortex neurons (Bair and Koch 1996; Berry et al. 1997; Buracas et al. 1998; Keat et al. 2001; Liu et al. 2001; Reich et al. 2001; Reich et al. 1997; Reinagel and Reid 2000, 2002; Victor 1999; Victor and Purpura 1998). The observed precision might be expected if strong spatially uniform stimuli evoked large synaptic currents synchronously at many synapses in the RGC. This could cause intracellular voltage to reach spike threshold rapidly, minimizing the effects of synaptic noise and other conductance fluctuations on the time of the next spike. This possibility is consistent with the finding that stronger stimuli produced lower spike time variability.

Several measures have been proposed for characterizing spike timing precision. A measure related to the one used here is the variability in the times of discrete firing "events" in sparse spike trains (Berry and Meister 1998; Berry et al. 1997; Keat et al. 2001; Liu et al. 2001; Mainen and Sejnowski 1995). This measure separates precision from reliability and yielded similar results in salamander and rabbit RGCs. However, although some portions of primate RGC spike trains could be decomposed into events, others contained local nonzero minima in firing rate (e.g., the period surrounding 0.3 s for the ON cell in Fig. 1*A*), complicating the estimation of event boundaries. Another measure of precision similar to the one used here is the width of Gaussian functions fitted to peaks in the firing rate time course (Reich et al. 1997; Reinagel and Reid 2000, 2002). This measure also separates precision from reliability and yielded comparable results in cat retina and LGN. However, it depends on a statistical (or arbitrary) assessment of the number of Gaussian functions required to fully specify the firing rate time course. A third measure is the smallest time bin size that affects the mutual information between the stimulus and spike train (Liu et al. 2001; Reinagel and Reid 2000). This makes no assumptions about the neural code and yielded similar results in cat LGN. However, mutual information estimates are subject to significant bias (Paninski 2003; Treves and Panzeri 1995), and standard methods of compensating for bias involve extrapolation from the data (Reinagel and Reid 2000; Strong et al. 1998). A related approach involves discriminating spike trains elicited by different stimuli using a metric that is sensitive to spike timing and examining the dependence of discriminability on this sensitivity (Reich et al. 2001; Victor 1999; Victor and Purpura 1997, 1998). This approach is best suited to discriminating a small number of discrete stimuli presented many times, rather than continuously varying stimuli with fewer repeats.

The measure of precision adopted here—the variability in the time of the first spike following a significant period of inactivity—indicated how precise RGC spike times can be using a simple analysis with few assumptions. Because this measure was only applicable at certain points in the spike train, it did not provide a measurement of precision for all stimuli. A similar caveat applies to previous studies, because each experiment probes a limited stimulus set. However, more elaborate precision measures could in principle account more fully for variation of precision with stimulus strength, and the importance of precision in communicating visual information to the brain.

Spike count variability and refractoriness in primate RGCs

Spike count variability exhibited large departures from Poisson statistics, in which the probability of a spike at any point in time depends only on the instantaneous firing rate and not on the times of previous spikes. Previous studies have shown spike count variability in RGCs of salamander, rabbit, and cat

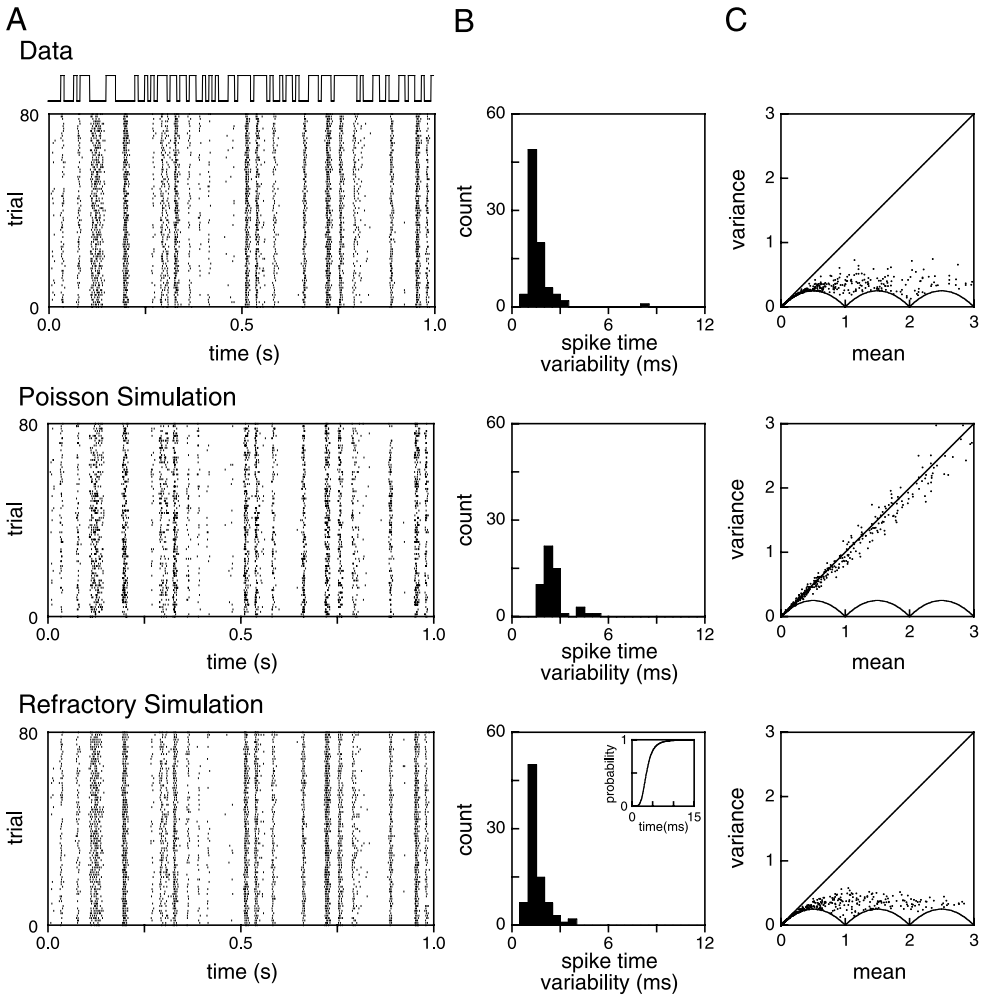

FIG. 7. Poisson and refractory simulations: ON cell. Rasters (*A*), spike time variability histograms (*B*), and spike count variance to mean relationship (*C*) are shown for a representative ON cell (*top*), a Poisson simulation (*middle*), and refractory simulation (*bottom*, see RESULTS and METHODS). The recovery function used in the simulation is shown in *B* (*inset*). The stimulus was spatially uniform binary noise with time course shown above the rasters and RMS contrast 96%. Histograms of spike time variability were computed in 0.5-ms bins. Spike count variance and mean were computed in 10-ms bins. Other details as in Figs. 2 and 4.

much lower than the mean, sometimes approaching the minimum variance possible with discrete counts (Berry and Meister 1998; Berry et al. 1997; Kara et al. 2000; Keat et al. 2001; Liu et al. 2001). One study of maintained activity in primate RGCs also revealed departures from Poisson statistics (Troy and Lee 1994). The large deviations from the Poisson prediction observed here are consistent with previous findings, and demonstrate that firing rate alone is an incomplete description of stimulus-driven responses.

Departures from Poisson statistics may be explained by the action potential refractory period which regularizes spike counts by reducing the probability of high counts (Berry and Meister 1998). Previous studies in salamander and cat have shown that the spike count variability of visual system neurons, including RGCs, is more accurately described by a refractory model with a free firing rate than by a time-varying Poisson process (Berry and Meister 1998; Kara et al. 2000; Liu et al. 2001). The present results confirm this in primate RGCs, suggesting that a free firing rate may adequately describe the visual signal that drives firing. However, more complex models could potentially provide a more accurate description. For example, the interval statistics of neurons in cat retina and LGN and monkey V1 cannot be entirely explained by a model with plausible refractory periods (Reich et al. 1998). Two other models have been proposed to reproduce the trial-to-trial variability of visual system neurons: the leaky integrate and fire model (Pillow et al. 2003; Reich et al. 1997) and a more elaborate model involving nonlinear feedback and two noise sources (Keat et al. 2001).

ON-OFF asymmetry

The observed ON-OFF asymmetries in spike time and count variability were approximately reproduced by the refractory simulation. The lower spike time variability of ON cells suggests that the ON pathway carries somewhat higher fidelity temporal signals to the brain. In one respect, this is surprising: the retinal OFF pathway starts out faster than the ON pathway due to the fast ionotropic glutamate receptors in OFF bipolars and the slower metabotropic receptors in ON bipolars (Nawy and Jahr 1990) and thus might be expected to signal rapid stimulus changes with more precisely timed spikes. However, the higher precision of ON cells is consistent with faster overall light response kinetics (Chichilnisky and Kalmar 2002), which

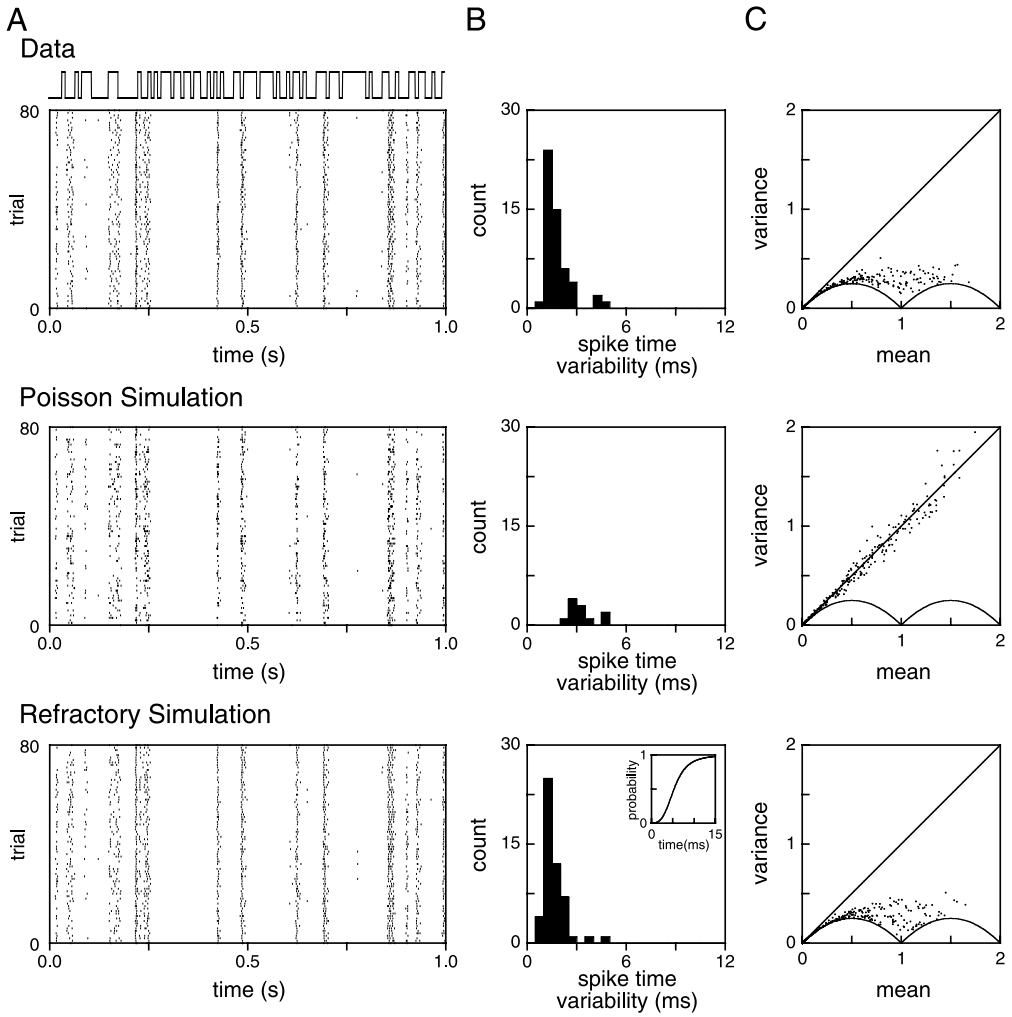

FIG. 8. Poisson and refractory simulations: OFF cell. Rasters (*A*), spike time variability histograms (*B*), and spike count variance to mean relationship (*C*) are shown for a representative OFF cell (*top*), Poisson simulation (*middle*), and refractory simulation (*bottom*). Other details as in Fig. 7.

may drive membrane potential to threshold more rapidly, reducing the influence of current fluctuations on the time of the spike. The lower count variability of ON cells for a given mean spike count (see Fig. 5*C*) may also result from faster firing rate modulations, which could cause responses to be more influenced by refractoriness within each time bin.

Consequences for visual signaling

The low spike count variability observed differs substantially from findings in primate visual cortex, where the variance approached or exceeded the mean (Bair and O'Keefe 1998; Barberini et al. 2000; Buracas et al. 1998; Gershon et al. 1998; McAdams and Maunsell 1999; Oram et al. 1999; Shadlen and Newsome 1998; Snowden et al. 1992; Softky and Koch 1993; Vogels et al. 1989; but see Gur et al. 1997). This is qualitatively consistent with a recent study that demonstrated lower variability in cat RGCs than in cortex (Kara et al. 2000). The higher variability in primate cortical neurons may be a consequence of noise in circuits downstream of the retina (Shadlen and Newsome 1998) or lower firing rates and shorter refractory periods in the cortex (Kara et al. 2000).

The finest spike timing precision observed in primate RGCs was comparable to or finer than that observed in neurons in cortical area MT (Bair and Koch 1996; Buracas et al. 1998). Because MT cells receive indirect inputs from hundreds or thousands of RGCs, higher precision might be expected in MT. The departure from this expectation may reflect three factors. First, noise in cortical neurons may limit precision, and common noise in cortical circuits may limit the ability to increase precision through pooling (Mazurek and Shadlen 2002; Shadlen and Newsome 1998). Second, precision depends on how strongly a stimulus drives firing, and the stimuli that drive MT neurons strongly differ from those that drive RGCs strongly. Third, direction selective cells in cortex could use the precise times of input spikes to extract the direction of motion and signal the results of this computation by gradual changes in firing rate, creating spike trains with higher timing variability. Therefore to meaningfully compare the spike timing precision of primate RGCs to that of MT neurons will require matched stimuli and an explicit model of the computations involved in creating direction-selective responses from retinal spike trains (Chichilnisky and Kalmar 2003).

ACKNOWLEDGMENTS

We thank E. Callaway for providing access to tissue; G. Horwitz, G. Field, F. Rieke, E. Callaway, T. Sejnowski for valuable input; A. Litke and colleagues for technology development; and S. Barry for technical assistance.

GRANTS

This work was supported by a Howard Hughes Predoctoral Fellowship, a National Institutes of Health SAIN training grant, a Merck Fellowship to V. J. Uzzell, National Eye Institute Grant EY-13150, a Sloan Research Fellowship, and a McKnight Scholar's Award to E. J. Chichilnisky.

REFERENCES

Bair W and Koch C. Temporal precision of spike trains in extrastriate cortex of the behaving macaque monkey. *Neural Comput* 8: 1185–1202, 1996.

Bair W and O'Keefe LP. The influence of fixational eye movements on the response of neurons in area MT of the macaque. *Vis Neurosci* 15: 779–786, 1998.

Barberini CL, Horwitz GD, and Newsome WT. A comparison of spiking statistics in motion sensing neurons of flies and monkeys. In: *Computational, Neural and Ecological Constraints of Visual Motion Processing*. Part V: *Neural Coding of Motion*, edited by Zeil J and Zanker JM. New York: Springer-Verlag, 2000, p. 307–320.

Berry MJ II and Meister M. Refractoriness and neural precision. *J Neurosci* 18: 2200–2211, 1998.

Berry MJ II, Warland DK, and Meister M. The structure and precision of retinal spike trains. *Proc Natl Acad Sci USA* 94: 5411–5416, 1997.

Buracas GT, Zador AM, DeWeese MR, and Albright TD. Efficient discrimination of temporal patterns by motion-sensitive neurons in primate visual cortex. *Neuron* 20: 959–969, 1998.

Chichilnisky EJ. A simple white noise analysis of neuronal light responses. *Network* 12: 199–213, 2001.

Chichilnisky EJ and Baylor DA. Receptive-field microstructure of blue-yellow ganglion cells in primate retina. *Nat Neurosci* 2: 889–893, 1999.

Chichilnisky EJ and Kalmar RS. Functional asymmetries in ON and OFF ganglion cells of primate retina. *J Neurosci* 22: 2737–2747, 2002.

Chichilnisky EJ and Kalmar RS. Temporal resolution of ensemble visual motion signals in primate retina. *J Neurosci* 23: 6681–6689, 2003.

Croner LJ, Purpura K, and Kaplan E. Response variability in retinal ganglion cells of primates. *Proc Natl Acad Sci USA* 90: 8128–8130, 1993.

Gershon ED, Wiener MC, Latham PE, and Richmond BJ. Coding strategies in monkey V1 and inferior temporal cortices. *J Neurophysiol* 79: 1135–1144, 1998.

Gur M, Beylin A, and Snodderly DM. Response variability of neurons in primary visual cortex (V1) of alert monkeys. *J Neurosci* 17: 2914–2920, 1997.

Huber PJ. *Robust Statistics.* New York: Wiley, 1981.

Kara P, Reinagel P, and Reid RC. Low response variability in simultaneously recorded retinal, thalamic, and cortical neurons. *Neuron* 27: 635–646, 2000.

Keat J, Reinagel P, Reid RC, and Meister M. Predicting every spike: a model for the responses of visual neurons. *Neuron* 30: 803–817, 2001.

Litke AM. The retinal readout system: a status report. *Nucl Instrum Methods Phys Res A* 435: 242–249, 1999.

Liu RC, Tzonev S, Rebrik S, and Miller KD. Variability and information in a neural code of the cat lateral geniculate nucleus. *J Neurophysiol* 86: 2789–2806, 2001.

Mainen ZF and Sejnowski TJ. Reliability of spike timing in neocortical neurons. *Science* 268: 1503–1506, 1995.

Mazurek ME and Shadlen MN. Limits to the temporal fidelity of cortical spike rate signals. *Nat Neurosci* 5: 463–471, 2002.

McAdams CJ and Maunsell JH. Effects of attention on the reliability of individual neurons in monkey visual cortex. *Neuron* 23: 765–773, 1999.

Meister M, Pine J, and Baylor DA. Multi-neuronal signals from the retina: acquisition and analysis. *J Neurosci Methods* 51: 95–106, 1994.

Nawy S and Jahr CE. Suppression by glutamate of cGMP-activated conductance in retinal bipolar cells. *Nature* 346: 269–271, 1990.

Oram MW, Wiener MC, Lestienne R, and Richmond BJ. Stochastic nature of precisely timed spike patterns in visual system neuronal responses. *J Neurophysiol* 81: 3021–3033, 1999.

Paninski L. Estimation of entropy and mutual information. *Neural Comput* 15: 1191–1254, 2003.

Pillow JW, Paninski L, and Simoncelli EP. Maximum likelihood estimation of a stochastic integrate-and-fire neural model. In: *Advances in Neural Information Processing Systems*, edited by Thrun S, Saul L, and Scholkopf B. Vancouver, British Columbia, Canada: MIT Press, 2004, vol. 16, p.1311–1318.

Polyak SL. *The Retina.* Chicago: University of Chicago Press, 1941.

Reich DS, Mechler F, and Victor JD. Temporal coding of contrast in primary visual cortex: when, what, and why. *J Neurophysiol* 85: 1039–1050, 2001.

Reich DS, Victor JD, and Knight BW. The power ratio and the interval map: spiking models and extracellular recordings. *J Neurosci* 18: 10090–10104, 1998.

Reich DS, Victor JD, Knight BW, Ozaki T, and Kaplan E. Response variability and timing precision of neuronal spike trains in vivo. *J Neurophysiol* 77: 2836–2841, 1997.

Reinagel P and Reid RC. Temporal coding of visual information in the thalamus. *J Neurosci* 20: 5392–5400, 2000.

Reinagel P and Reid RC. Precise firing events are conserved across neurons. *J Neurosci* 22: 6837–6841, 2002.

Rosner B. *Fundamentals of Biostatistics.* Belmont: Duxbury Press, 1995.

Schnapf JL, Nunn BJ, Meister M, and Baylor DA. Visual transduction in cones of the monkey Macaca fascicularis. *J Physiol* 427: 681–713, 1990.

Shadlen MN and Newsome WT. The variable discharge of cortical neurons: implications for connectivity, computation, and information coding. *J Neurosci* 18: 3870–3896, 1998.

Snowden RJ, Treue S, and Andersen RA. The response of neurons in areas V1 and MT of the alert rhesus monkey to moving random dot patterns. *Exp Brain Res* 88: 389–400, 1992.

Softky WR and Koch C. The highly irregular firing of cortical cells is inconsistent with temporal integration of random EPSPs. *J Neurosci* 13: 334–350, 1993.

Strong SP, Koberle R, de Ruyter van Steveninck R, and Bialek W. Entropy and Information in neural spike trains. *Phys Rev Lett* 80: 197–200, 1998.

Sun H, Ruttiger L, and Lee BB. The spatiotemporal precision of ganglion cell signals: a comparison of physiological and psychophysical performance with moving gratings. *Vision Res* 44: 19–33, 2004.

Treves A and Panzeri S. The upward bias in measures of information derived from limited data samples. *Neural Comput* 7: 399–407, 1995.

Troy JB and Lee BB. Steady discharges of macaque retinal ganglion cells. *Vis Neurosci* 11: 111–118, 1994.

Victor JD. Temporal aspects of neural coding in the retina and lateral geniculate. *Network* 10: R1–R66, 1999.

Victor JD and Purpura KP. Metric-space analysis of spike trains: theory, algorithms and application. *Network Comput Neural Syst* 8: 127–164, 1997.

Victor JD and Purpura KP. Spatial phase and the temporal structure of the response to gratings in V1. *J Neurophysiol* 80: 554–571, 1998.

Vogels R, Spileers W, and Orban GA. The response variability of striate cortical neurons in the behaving monkey. *Exp Brain Res* 77: 432–436, 1989.